Temperature Profile Retrieval by Two-Dimensional Filtering

K. S. NATHAN,* P. W. ROSENKRANZ AND D. H. STAELIN

Research Laboratory of Electronics, Massachusetts Institute of Technology, Cambridge, MA 02139

(Manuscript received 28 March 1984, in final form 20 December 1984)

ABSTRACT

Satellite-borne radiometers have been used with increasing success to monitor geophysical parameters. The majority of the statistical retrieval schemes currently in use for estimating atmospheric temperature profiles are one-dimensional (1-D), that is, they consider correlations only in the dimension perpendicular to the surface. Here, a two-dimensional (2-D) spatial filter, optimum in the minimum-mean-square error sense, is used to retrieve atmospheric temperature profiles from Microwave Sounder Unit measurements. Horizontal correlations along the orbital track are taken into account. This additional statistical information results in lower mean-square errors for the 2-D filter compared to that of its 1-D counterpart. The previously unstudied behavior of retrieval errors as a function of spatial frequency along the orbital track is also investigated. A large part of the improved performance of the 2-D filter is due to the reduction of short spatial wavelength components in the error. In addition, retrievals were carried out over a severe cold front. The 2-D technique yielded substantially lower errors than the 1-D approach. The latter does not perform so well over fronts because of the loss in vertical correlation due to the presence of layers of air with different lapse rates.

1. Introduction

The problem of estimating temperature profiles in the atmosphere by means of a passive radiometer can be viewed as inversion of the equation of radiative transfer. The latter relates atmospheric temperature to the power observed by the radiometer (the antenna temperature spectrum). Statistical techniques utilizing correlations in the vertical domain alone have been widely implemented (e.g., see Rodgers, 1976; Smith and Woolf, 1976). It was shown by Ledsham and Staelin (1978) and Toldalagi (1980) that two-dimensional filtering could produce significant reductions in retrieval errors. Similar concepts have been applied by Pokrovsky and Ivanykin (1978).

In this paper we discuss, in both real and transform space, the results of a two-dimensional spatial filter which is optimum (for stationary statistics) in the minimum-mean square error sense (see also Nathan, 1983; Rosenkranz, 1982). This approach considers correlations both in the vertical and horizontal (along the orbital track) directions. We used data from the TIROS-N and NOAA-6 Microwave Sounding Units (MSU) which measure the 60 GHz oxygen resonance band. This instrument is described by Smith *et al.* (1979). Our purpose is, first, to confirm the utility of spatial filtering with the MSU instrument, and second, to investigate the origin of the improvement, particularly its horizontal scale.

* Current address: Jet Propulsion Laboratory, California Institute of Technology, Pasadena, CA 91109.

2. Formulation

The two-dimensional temperature estimate can be expressed as:

$$\hat{\mathbf{T}}(x) = \mathbf{D}(x)*[\mathbf{T}_A(x) - \bar{\mathbf{T}}_A(x)] + \bar{\mathbf{T}}(x) \qquad (1)$$

where $\mathbf{T}_A(x)$ is a column vector composed of measured antenna temperatures. We used three of the MSU channels, listed in Table 1. Here $\bar{\mathbf{T}}_A(x)$ is the mean of $\mathbf{T}_A(x)$, $\hat{\mathbf{T}}(x)$ the estimated temperature profile, $\bar{\mathbf{T}}(x)$ the mean temperature profile and $\mathbf{D}(x)$ is the optimal estimator, hereafter referred to as the D matrix; x is the variable along the orbital track and the asterisk denotes matrix convolution. We arrive at the optimal filter by requiring the estimate error ($\hat{\mathbf{T}} - \mathbf{T} = \mathbf{e}$) to be uncorrelated with the measured data $\mathbf{T}_A$:

$$E[(\hat{\mathbf{T}} - \mathbf{T}) \cdot (\mathbf{T}_A - \bar{\mathbf{T}}_A)] = 0$$

where $\mathbf{T}$ is the atmospheric temperature obtained from the National Meteorological Center (NMC) gridded analysis, and $E[\ ]$ denotes the expected value operator. The resulting D matrix is then

$$\mathbf{D}(x) = \mathbf{R}_{ta}(x)*\mathbf{R}_{aa}^{-1}(x). \qquad (2)$$

Here $\mathbf{R}_{ta}(x)$ is the *a priori* cross-correlation matrix of temperature with antenna temperature and $\mathbf{R}_{aa}(x)$ is the *a priori* antenna temperature autocorrelation matrix. Here, we have assumed that these matrices are functions of spatial lags only and independent of longitude and latitude, i.e., that the associated processes are stationary. Hence we obtain a filter of the Wiener type as discussed by Rosenkranz (1978),

TABLE 1. Microwave Sounder Unit weighting functions.

Channel number	Frequency (GHz)	Pressure level of peak (mb)
2	53.73	600
3	54.96	270
4	57.95	80

rather than of the Kalman type as described by Ledsham and Staelin (1978).

The speed and efficiency of the fast Fourier transform algorithm make it ideal for computation of spectra. Therefore, we replace Eq. (2) by the formulation in the spatial frequency domain (u):

$$\mathbf{D}(u) = \mathbf{S}_{ta}(u) \cdot \mathbf{S}_{aa}^{-1}(u), \tag{3}$$

where $\mathbf{S}_{ta}(u)$ and $\mathbf{S}_{aa}(u)$ are the cross spectrum and energy spectrum matrices corresponding to $\mathbf{R}_{ta}(x)$ and $\mathbf{R}_{aa}(x)$. It follows that the estimate of temperature deviation from the mean is now of the form

$$\hat{\mathbf{T}}(u) = \mathbf{D}(u) \cdot \mathbf{T}_A(u), \tag{4}$$

where $\hat{\mathbf{T}}(u)$ and $\mathbf{T}_A(u)$ are Fourier transforms of the temperature estimate and the antenna temperatures respectively, both with mean values subtracted.

The required spectra, $\mathbf{S}_{ta}(u)$ and $\mathbf{S}_{aa}(u)$, were estimated using the periodogram approach over dataset A: 109 orbits from the periods 2–8 July 1979 (TIROS-N) and 9–13 February 1981 (NOAA-6). These orbits were selected from a larger dataset by excluding any orbits with data gaps. We did no screening for clouds, although rain clouds do perturb the measured antenna temperatures, which tends to reduce their correlation with atmospheric temperature. Because the discrete Fourier transform is defined over one period of an implicitly periodic sequence, it was necessary to use data sequences that started and ended at locations that have approximately the same physical conditions. TIROS-N is in a polar orbit, but we used only Northern Hemisphere semiorbits. Each semiorbit contained 128 measurements, spaced at intervals of 168 km. The NMC analysis was interpolated bilinearly in time and space to the locations of the satellite measurements. The temperatures within ~10° of the equator are fairly constant around the globe, and hence do not introduce any discontinuities at the end points of the Northern Hemisphere semiorbits.

3. Retrieval errors

a. Error total energy

We shall compare the performance of the two-dimensional (2-D) filter to that of its (1-D) counterpart. The 1-D filter was simulated using the 2-D formulation for the sake of consistency. This was done by computing **D** in the frequency domain with flat spectra, corresponding to the impulsive correlation functions of the 1-D case. Retrieval error statistics were computed from two datasets: the training dataset (A) and dataset B, which contained 78 orbits of TIROS-N data from the period 10–18 October 1979. We divided the Northern Hemisphere into three zones, 0–30°, 30–60° and 60–90° latitude. The rms errors for these three zones are plotted as functions of pressure in Figs. 1–3. Mean errors are included in Figs. 1–3; however, at most levels in dataset B and all levels in dataset A they contribute a minor part of the error energy.

In all zones and levels, when errors are computed from the training dataset (A), the 2-D filter produces lower errors than the 1-D. This is expected inasmuch as the addition of *a priori* information (horizontal correlations) cannot increase errors provided that the information is optimally used. On the test dataset (B) the 2-D filter does as well or better than the 1-D in most cases, although the margin of improvement is generally lower, and near the tropical tropopause (~100 mb) the 2-D actually does significantly worse. At least three effects contribute to this difference between datasets.

1) The datasets with which we are working are fairly small for the purpose of determining the 2-D coefficients; in this case each orbit provides only one element of the statistical ensemble for each spatial frequency and level in the energy spectra. Furthermore, these elements are not chosen in an independent manner, but from (usually) consecutive orbits.

2) Dataset B represents a different season than the two seasons which were combined in dataset A. In other words, the coefficients in the D matrix are

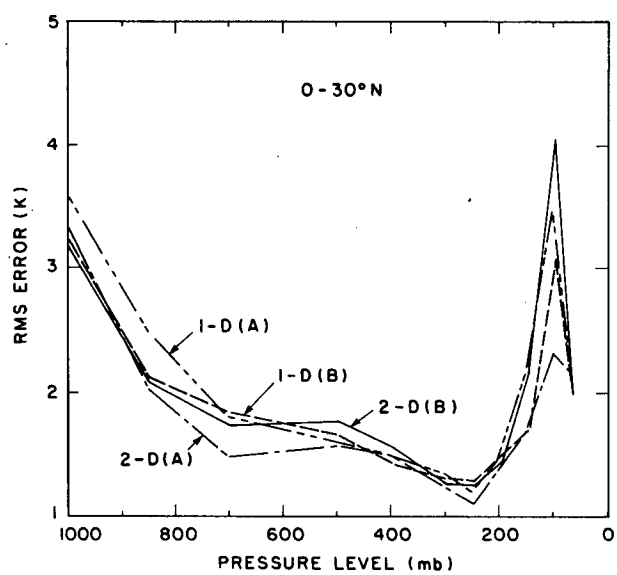

FIG. 1. Root-mean-square temperature errors for 1-D and 2-D retrievals compared with the NMC analysis, 0–30° latitude. Error statistics are plotted for the training dataset (A) and the test dataset (B).

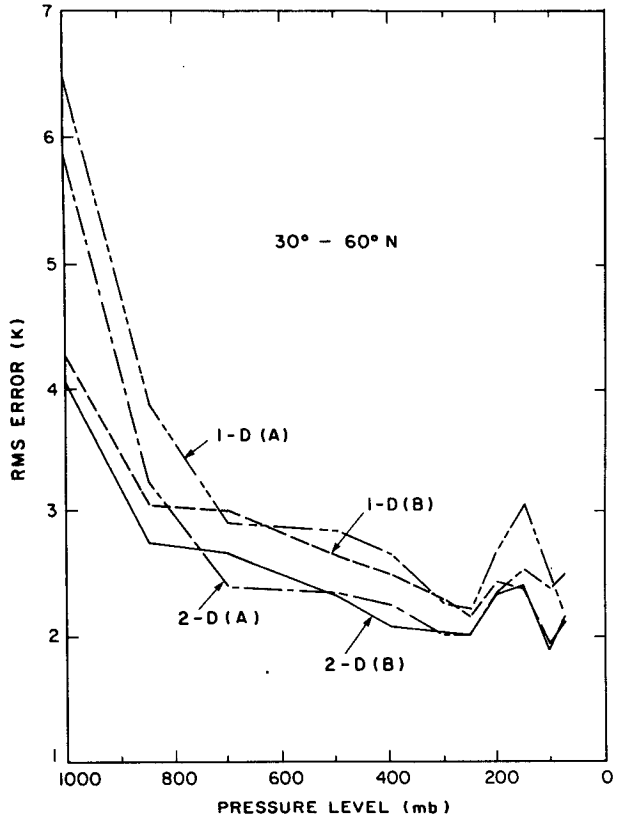

FIG. 2. As in Fig. 1 but for 30–60° latitude.

"tuned" to dataset A rather than to dataset B. If larger datasets had been used, and the test dataset were more compatible with the training dataset, we would expect to see more nearly the same results from the two.

3) Since we are using actual MSU measurements rather than simulations, any errors in the NMC analysis contribute to the "retrieval error." It may be significant that Fig. 2, for the 30–60° zone, which is more densely sampled by radiosondes than the other two zones, shows the most consistent (between datasets A and B) improvement from the 2-D filter (except near the surface, which may be attributed to a larger *a priori* variance in dataset A). However, the differences between the midlatitude zone on the one hand, and the tropical and polar zones on the other, might also be produced by different climatologies of the latter in the sense that although horizontal correlations of temperature are present there, they might yield lesser advantage *vis-à-vis* vertical correlations.

Despite these caveats, the most significant result that we find in Figs. 1–3 is that the 2-D filter produces lower errors than the 1-D, and this improvement persists (in general) when the D matrix is applied to data completely distinct from those from which it was derived. Our conclusion is that horizontal correlations of atmospheric temperature provide additional information about vertical structure, in the context of remote sounding.

b. *Horizontal spectra of the retrieval errors*

The error spatial frequency behavior is defined by Rosenkranz (1978):

$$\mathbf{S}_e(u) = \mathbf{S}_{tt}(u) - \mathbf{D}(u)\mathbf{S}_{ta}^{\mathrm{T}}(u) + \mathbf{D}(u)\mathbf{S}_{aa}(u)\mathbf{D}^{\mathrm{T}}(u) - \mathbf{S}_{ta}(u)\mathbf{D}^{\mathrm{T}}(u) \quad (5)$$

The error energy spectrum of level i, $S_{eii}(u)$, is defined as the Fourier transform of the autocorrelation of the retrieval error; and $\mathbf{S}_{tt}(u)$ is the energy spectrum of temperature $\mathrm{T}(x)$.

In Fig. 4 we have divided the spatial frequency spectrum into six bands and integrated to determine the error energy contribution of each one of these bands to both one- and two-dimensional filter errors, using dataset B. As one would expect, the majority of the error energy is concentrated at long wavelengths. In fact, there is very little or no energy at wavelengths less than 840 km. We notice that at lower atmospheric levels the energy at short wavelengths is relatively greater. This is in accordance with the temperature variation at these levels. The temperature is more smoothly behaved horizontally at higher altitudes while at the surface we see more short-distance effects.

At very low frequencies (long wavelengths, band 1) there is virtually no difference in error energy between the 1-D and 2-D techniques. From frequency

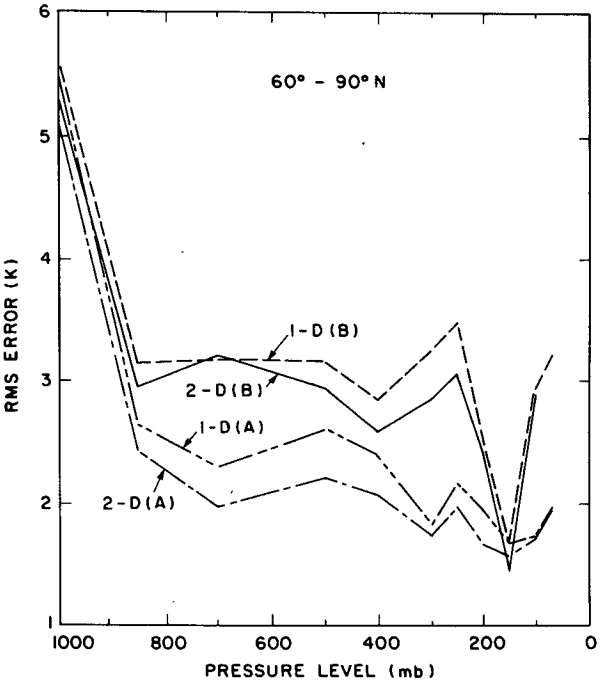

FIG. 3. As in Fig. 1 but for 60–90° latitude.

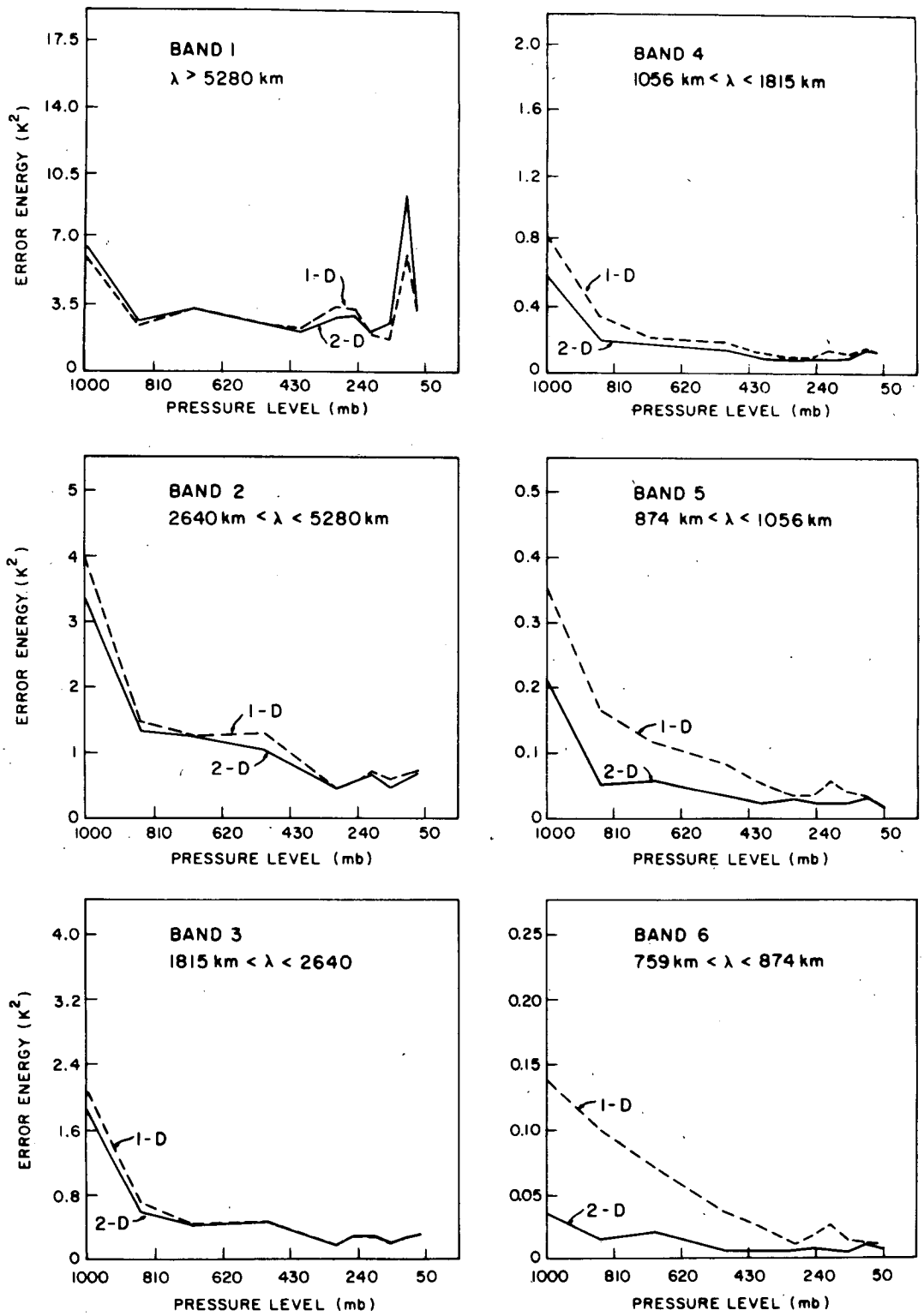

FIG. 4. Temperature error energy in six wavelength bands (Northern Hemisphere, dataset B).

band 2 onward the 2-D filter improves its performance relative to the purely vertically tuned filter—particularly in the troposphere. As we move to shorter wavelengths, this improvement is clearly enhanced. For wavelengths shorter than 1800 km (band 4 and up) the 2-D filter results in lower errors throughout

all pressure levels. This decrease in error continues at still shorter wavelengths (band 6); however, the energy decreases significantly and its contribution to the overall rms error becomes minimal.

The sensor noise is only a few tenths of a degree Kelvin, and its reduction by virtue of horizontal averaging is not a significant cause of the 2-D filter's improvement (Nathan, 1983). The latter is therefore attributed to the additional information along the orbital track. Figure 5 shows a typical correlation function computed from the *a priori* dataset. The horizontal correlation function is nonnegligible out to ~1500–2000 km. It is this added information that renders the 2-D filter more effective at those particular wavelengths. At longer spatial lags the correlation functions are too small to add much information. Although horizontal correlations of the scale shown in Fig. 5 are supported by several independent studies (e.g., Hillger and Vander Haar, 1979), we should note that they would be present in the NMC analysis, if only by virtue of the optimal interpolation method used to do the analysis (Bergman, 1979).

Alternatively, the improvement can be regarded as a result of low-pass spatial filtering. Since the correlation functions are of nonzero extent, the corresponding 2-D D matrix has finite width in the frequency domain. From Eq. (4) it follows that spatial frequency components in T_a above a certain cutoff point are highly attenuated. In contrast, the 1-D D matrix, which is an impulse in the spatial domain, is constant across the frequency spectrum and thereby weights higher frequencies as much as lower ones. Such high-frequency components in the antenna temperature often arise from spurious sources. These spurious sources include sudden discontinuities in the antenna temperature due to factors such as changes in emissivity due to land or ice boundaries, sudden increases in surface elevation (mountain ranges), etc. It is generally these artificial effects that constitute short wavelength phenomena. Therefore, their elimination by the 2-D filter results in more accurate retrievals.

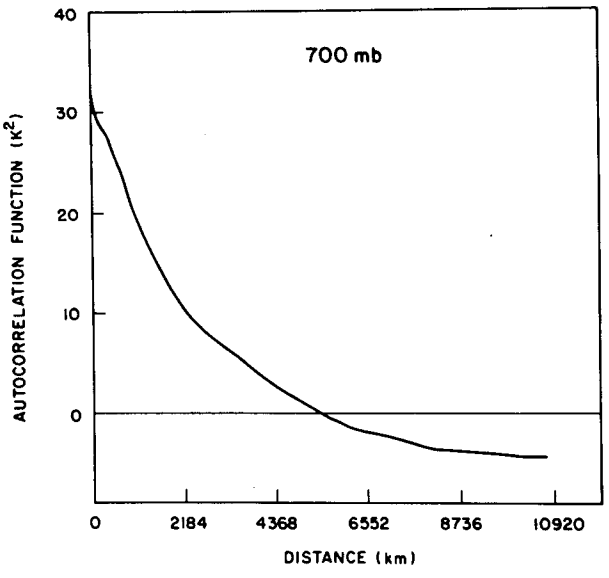

FIG. 5. Autocorrelation function of NMC temperature at 700 mb.

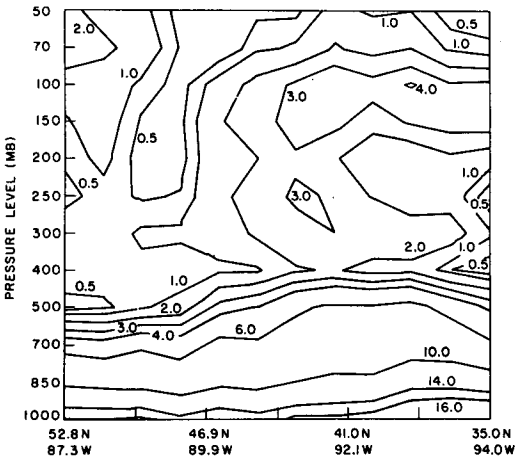

FIG. 6. Temperature errors as a function of pressure level and location along the satellite track, for the 1-D retrieval.

The results in the upper troposphere and stratosphere, on the other hand, are little affected by surface effects on the 53.73 GHz channel. Yet, as Fig. 4 indicates, there is also significant improvement at these levels with the 2-D filter. The explanation is that some of the information provided by horizontal correlation statistics is not available through vertical correlation statistics alone.

4. Case study: Retrieval over a storm front

Having compared the overall performance of the 2-D and 1-D filters, we now turn our attention to a specific case, namely, a strong cold front over the midwestern United States and Canada on 11 February 1981. We observe a substantial improvement in the retrieval errors in the troposphere when the horizontal dimension is taken into consideration. This improvement also extends to the stratosphere but on a somewhat more modest scale. The contour plots in Figs. 6 and 7 illustrate this. Here, data over the storm from a single orbit are used. The abscissas correspond to the movement of the satellite along the orbital track, which was roughly parallel to the front and on the cold side (at the surface). The vertical scale is pressure and the curves are of equal absolute error (isoerrors). There is an appreciable reduction in the absolute error for the 2-D case in the troposphere. At 500 mb the 1-D formulation results in errors ranging up to 5 K. The maximum error at this level for the 2-D filter is of the order of 2–3 K. In the stratosphere the effect of the added dimension is less marked. There is a definite improvement (via the 2-D method)

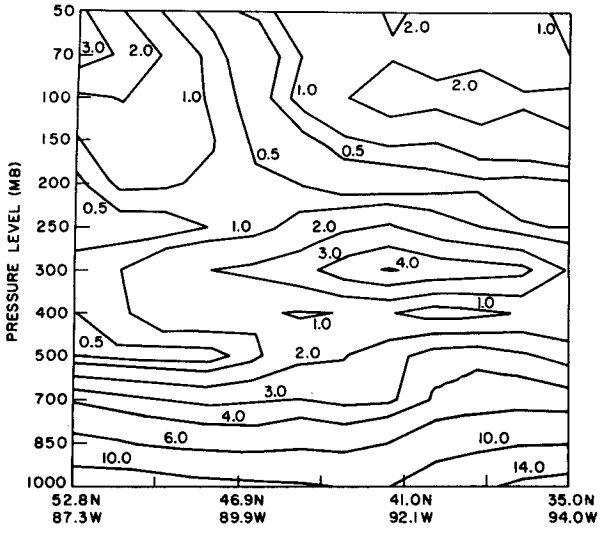

FIG. 7. As in Fig. 6 but for the 2-D retrieval.

south of 47°N. However, this is not true at the beginning of the data sample.

It is clear from the above results that the 1-D filter performs worse than the 2-D filter in the troposphere. This is in large part due to the loss of vertical correlation over such fronts. The colder polar air is characterized by a temperature profile different than that of warmer air. At the front this results in two layers of air with different lapse rates. The 2-D filter relies on additional information in the horizontal domain to offset this effect.

The surface and lower troposphere errors are unusually high, as indicated by the error contour plots. Figure 8 shows the 850 mb level retrievals over the semiorbit for both filters. The deviation of the temperatures from the mean values is given in degrees Kelvin. Comparing the two retrievals we note that the 2-D filter sharpens the response over the storm front ~(48°N, 89°W). This sharpening is due to statistical filtering, i.e., the presence of horizontally correlated information as opposed to "smoothing" due to horizontal averaging. The latter in the limiting case would have the sole effect of eliminating sensor noise.

The errors over the storm in the Western Hemisphere from 30 to 60°N are definitely higher than the errors in most other parts of the orbit. In both cases the temperature estimate is warmer than the NMC analysis verification data. This implies that the antenna temperature for channel 1 (53.73 GHz), with a weighting function which peaks near 850 mb, might be warmer than it "should" be. This is the reverse of what one might expect because rain or heavy clouds typically attenuate the power seen by the radiometer and decrease the antenna temperature. One means of validating the measured antenna temperatures is to compare them with simulated ones based on the NMC analysis. Given the physical temperature profile T (NMC analysis) and the weighting function $\mathbf{C}$, the expected antenna temperature $T_{A(\mathrm{NMC})}$ can be computed:

$$T_{A(\mathrm{NMC})} = \mathbf{C}^{\mathrm{T}}\mathbf{T}. \tag{6}$$

The measured data are compared to the calculated brightness temperatures in Fig. 9, and are precisely what we would expect, particularly over the storm region; i.e., the radiometer is responding just as expected to the atmospheric conditions. This conclusion agrees with the study of MSU data done by Grody (1983) in the case of fields of view which do not contain rain.

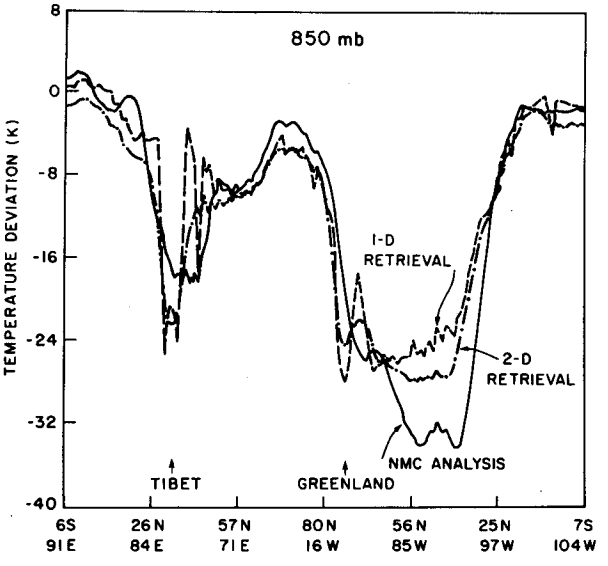

FIG. 8. Temperature deviation from the mean at 850 mb versus location. The analysis is compared with two retrievals.

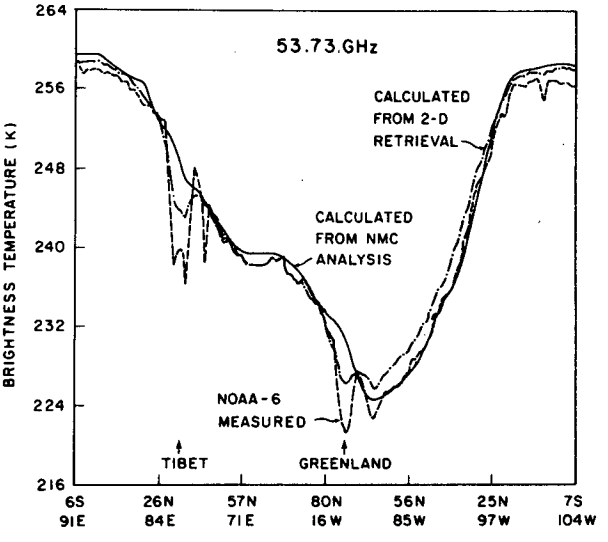

FIG. 9. Comparison of calculated and measured brightness temperatures at 53.73 GHz.

We can then infer that our statistical estimator is not optimal for these data. This can be experimentally verified. The antenna temperature for this particular channel can also be calculated using the retrieved temperature as ground truth,

$$T_{A(\text{ret})} = \mathbf{C}^{\mathrm{T}}\hat{\mathbf{T}}. \tag{7}$$

We might expect $T_{A(\text{ret})}$ to be substantially warmer than $T_{A(\text{NMC})}$ since $\hat{T} > T$ for the levels in question. Figure 9 also compares $T_{A(\text{ret})}$ with the measured antenna temperature. The former is only slightly warmer than the observed data over the area of the storm. In fact, a difference in temperature of over 10 K results in a variation in the antenna temperature of only about 1.5 K. We can formulate this in a more quantitative manner: Let

$$\hat{\mathbf{T}} = \mathbf{T} + \mathbf{e}, \tag{8}$$

where $\mathbf{e}$ is the difference between the retrieved and actual temperatures. Substituting (8) in (7) gives:

$$T_{A(\text{ret})} = T_{A(\text{NMC})} + \mathbf{C}^{\mathrm{T}}\mathbf{e}. \tag{9}$$

But the antenna temperatures computed from the retrieved data are very close to those computed via the ground truth:

$$T_{A(\text{NMC})} \approx T_{A(\text{ret})} = T_{A(\text{NMC})} + \mathbf{C}^{\mathrm{T}}\mathbf{e}. \tag{10}$$

Therefore, $\mathbf{C}^{\mathrm{T}}\mathbf{e} \approx 0$, i.e., $\mathbf{e}$ belongs to the null space of $\mathbf{C}$. Since $\mathbf{D}$ is essentially performing the inverse of the weighting function operation, it follows that the retrieval error lies in the orthogonal complement of the range space of the estimator $\mathbf{D}$. In other words, the error cannot be reached by means of $\mathbf{D}$. This merely restates that the *a priori* statistics used to calculate the estimate are not representative of those characterizing the storm front under study.

The temperature profile at the point 52.8°N, 87.3°W is plotted in Fig. 10. We notice a major temperature inversion in the lower troposphere. The 700 mb level is warmer than the surface. This explains the warmer radiometer temperatures for channel 2. Clearly, the extent of this inversion makes the *a priori* vertical statistics inappropriate. Nevertheless, the 2-D filter fares far better than the 1-D.

Finally, in Fig. 9 there are several narrow features in the measured antenna temperature. The first occurs in the vicinity of 32°N, 82°E and the second around 75°N, 58°W. The former is over Tibet, which is at a considerable surface elevation, and the latter is over Greenland, where an increase in the reflectivity combined with a greater surface elevation could have caused the sudden drop in the antenna temperature. In both instances the 2-D filter is less sensitive to these perturbations and hence produces a more accurate temperature retrieval (Fig. 8). In Fig. 8 we see that the 1-D inversion is very erratic over the Tibetan plateau region. The 2-D filter, on the other hand, smooths the retrieval as a result of horizontal correlations and is less prone to errors. The correlation functions in the 1-D case are impulses at the origin as is the corresponding D matrix. Therefore, the convolution operation with the measured data reproduces any pulselike features of the antenna temperature. The 2-D horizontal correlation functions, however, have finite width both in the spatial frequency and space domains. This characteristic is naturally preserved in the D matrix. From (1), it is clear that any pulse in T_A will be smoothed (or broadened) by the filter. Since such sharp discontinuities are rarely due to atmospheric temperature this filtering also results in more accurate retrievals.

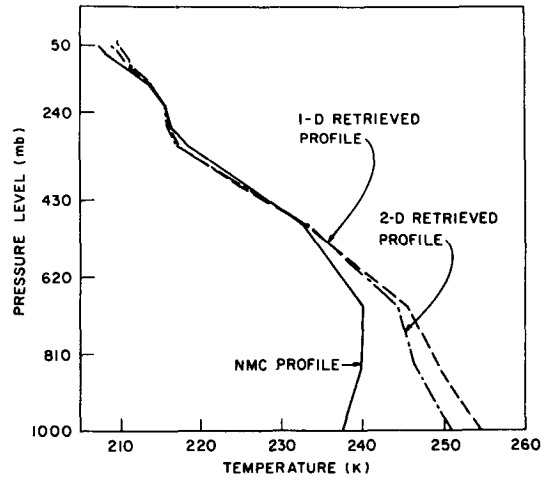

FIG. 10. Temperature vertical profiles at 52.8°N, 87.3°W.

5. Summary and suggestions for further research

We have developed, implemented, and tested a two-dimensional spatial filter for the retrieval of temperature profiles in the atmosphere. The formulation made use of correlations both in the horizontal and vertical domains. Its performance was compared to that of a 1-D technique. Lower retrieval errors result from the 2-D version, especially in the troposphere. The additional horizontal information used in the 2-D formulation substantially improved temperature retrievals over a severe cold front where vertical correlations are lessened. The effective reduction of instrument noise as a major source of the 2-D technique's improvement was ruled out. The improved results of the 2-D filter in the upper troposphere point to the presence of profile components in the null space of the weighting functions that are horizontally correlated with the observed data.

The 2-D technique also enables us to study the behavior of the parameters of interest in the horizontal dimension in both spatial and transform domains. This allowed us to examine the effect of the autocorrelation function width on the retrieval errors and their corresponding spectra. The spatial frequency

analysis revealed the effectiveness of the 2-D filter in reducing high-frequency components of the error. These shorter wavelength terms often arise due to spurious features in the data, such as abrupt changes in the surface elevation or emissivity, and are filtered out in the 2-D approach.

The 2-D technique has some disadvantages. First, it obviously involves more data processing. Second, the present implementation of the 2-D filter does not allow for regionalization of the statistics. For the same reason, we cannot differentiate between land and ocean areas where the change in emissivity might cause larger errors near the surface.

We found that the 2-D method performed better over a cold front because the 1-D technique suffered from a loss of vertical correlation. Both techniques resulted in larger than usual errors at the surface over this severe front. The large errors were the result of the temperature inversion shown in Fig. 10. The use of surface temperature information from concurrent ground-based observations would no doubt have lessened these errors, but use of such auxiliary information was not considered in our algorithms. The MSU sounder has only one channel (other than the unused window channel) that responds to this region of the troposphere. Finer sampling of this section of the atmosphere could better resolve temperature inversions.

A natural extension of the 2-D filter would be to incorporate the additional y direction, along the surface perpendicular to the satellite track. This can be achieved by taking into account other scan angles (only the nadir angle was used here), thus yielding a three-dimensional formulation. However, the 2-D Fourier transform operation cannot be performed along the "x" and "y" directions because the antenna spot patterns on the earth differ for each scan angle. Consequently, the cross-correlation between the different scan positions should be treated in the same manner as those between the pressure levels. The maximum correlation lag one can obtain in the y dimension is of the order of 2200 km. Figure 4 plots the retrieval error energy for that band (band 3). The error energy is well over 1 K^2 in the lowest troposphere and we can expect that the additional correlation would reduce it.

Acknowledgments. This research was supported by National Aeronautics and Space Administration Grant NAG5-10 and National Oceanic and Atmospheric Administration Grants 04-8-MO1-1 and NA84AA-D-00001.

REFERENCES

Bergman, K., 1979: A multivariate optimum interpolation analysis system of temperature and wind fields. *Mon. Wea. Rev.*, **107,** 1423–1444.

Grody, N. C., 1983: Severe storm observations using the Microwave Sounding Unit. *J. Climate Appl. Meteor.*, **22,** 609–625.

Hillger, D. W., and T. H. Vonder Haar, 1979: An analysis of satellite infrared soundings at the mesoscale using statistical structure and correlation functions. *J. Atmos. Sci.*, **36,** 287–305.

Ledsham, W. H., and D. H. Staelin, 1978: An extended Kalman–Bucy filter for atmospheric temperature profile retrieval with a passive microwave sounder. *J. Appl. Meteor.*, **17,** 1023–1033.

Nathan, K. S., 1983: Application of a multi-dimensional spatial filter to temperature profile retrieval. S.M. thesis, EECS Dept., MIT, 173 pp.

Pokrovsky, O. M., and E. E. Ivanykin, 1978: Spatial analysis of temperature and geopotential fields on the basis of data from remote sounding of the atmosphere. *Z. Meteor.*, **28,** 3–14.

Rodgers, C. D., 1976: Retrieval of atmospheric temperature and composition from remote measurements of thermal radiation. *Rev. Geophys. Space Phys.*, **14,** 609–624.

Rosenkranz, P. W., 1978: Inversion of data from diffraction-limited multiwavelength remote sensors, 1. Linear case. *Radio Sci.*, **13,** 1003–1010.

——, 1982: Inversion of data from diffraction-limited multiwavelength remote sensors, 3. Scanning multichannel microwave radiometer data. *Radio Sci.*, **17,** 257–267.

Smith, W. L., and H. M. Woolf, 1976: The use of eigenvectors of statistical covariance matrices for interpreting satellite sounding radiometer observations. *J. Atmos. Sci.*, **33,** 1127–1140.

——, ——, C. M. Hayden, D. Q. Wark and L. M. McMillin, 1979: The TIROS-N Operational Vertical Sounder. *Bull. Amer. Meteor. Soc.*, **60,** 1177–1187.

Toldalagi, P. M., 1980: Adaptive filtering methods applied to satellite remote-sensing of the atmosphere for meteorological purposes. Ph.D. thesis, EECS Dept, MIT, 230 pp.